JCI The Journal of Clinical Investigation

Extracellularly occurring histone H1 mediates the binding of thyroglobulin to the cell surface of mouse macrophages.

K Brix, … , F Lottspeich, V Herzog

J Clin Invest. 1998;102(2):283-293. https://doi.org/10.1172/JCI1614.

Research Article

Thyroglobulin is the major secretory protein of thyroid epithelial cells. Part of thyroglobulin reaches the circulation of vertebrates by transcytosis across the epithelial wall of thyroid follicles. Clearance of thyroglobulin from the circulation occurs within the liver via internalization of thyroglobulin by macrophages. Here we have analyzed the interaction of thyroglobulin with the cell surface of J774 macrophages with the aim to identify the possible thyroglobulin-binding sites on macrophages. Binding of thyroglobulin to J774 cells was saturated at approximately 100 nM thyroglobulin with a Kd of 50 nM, and it was competed by the ligand itself. Preincubation of J774 cells with thyroglobulin resulted in downregulation of thyroglobulin-binding sites, indicating internalization of thyroglobulin and its binding proteins. By affinity chromatography, two proteins from J774 cells were identified as thyroglobulin-binding proteins with an apparent molecular mass of approximately 33 kD. Unexpectedly, both proteins were identified as histone H1 by protein sequencing. The occurrence of histone H1 at the plasma membrane was further proven by biotinylation or immunolabeling of J774 cells. The in vitro interaction between histone H1 and thyroglobulin was analyzed by surface plasmon resonance that revealed a Kd at 46 nM. In situ, histone H1 was colocalized to FITC-Tg-containing endocytic compartments of Kupffer cells, i.e., liver macrophages. We conclude that histone H1 is detectable at the cell surface of macrophages where […]

Find the latest version:

https://jci.me/1614/pdf

Extracellularly Occurring Histone H1 Mediates the Binding of Thyroglobulin to the Cell Surface of Mouse Macrophages

Klaudia Brix,* Wolfgang Summa,* Friedrich Lottspeich,‡ and Volker Herzog*

**Institut für Zellbiologie and Bonner Forum Biomedizin, Universität Bonn, D-53121 Bonn, Germany; and ‡Max-Planck-Institut für Biochemie, Proteinanalytik, Am Klopferspitz, D-82152 Martinsried (bei München), Germany*

Abstract

Thyroglobulin is the major secretory protein of thyroid epithelial cells. Part of thyroglobulin reaches the circulation of vertebrates by transcytosis across the epithelial wall of thyroid follicles. Clearance of thyroglobulin from the circulation occurs within the liver via internalization of thyroglobulin by macrophages. Here we have analyzed the interaction of thyroglobulin with the cell surface of J774 macrophages with the aim to identify the possible thyroglobulin-binding sites on macrophages. Binding of thyroglobulin to J774 cells was saturated at ~ 100 nM thyroglobulin with a K_d of 50 nM, and it was competed by the ligand itself. Preincubation of J774 cells with thyroglobulin resulted in downregulation of thyroglobulin-binding sites, indicating internalization of thyroglobulin and its binding proteins. By affinity chromatography, two proteins from J774 cells were identified as thyroglobulin-binding proteins with an apparent molecular mass of ~ 33 kD. Unexpectedly, both proteins were identified as histone H1 by protein sequencing. The occurrence of histone H1 at the plasma membrane was further proven by biotinylation or immunolabeling of J774 cells. The in vitro interaction between histone H1 and thyroglobulin was analyzed by surface plasmon resonance that revealed a K_d at 46 nM. In situ, histone H1 was colocalized to FITC-Tg–containing endocytic compartments of Kupffer cells, i.e., liver macrophages. We conclude that histone H1 is detectable at the cell surface of macrophages where it serves as a thyroglobulin-binding protein and mediates thyroglobulin endocytosis. (*J. Clin. Invest.* 1998. 102:283–293.) Key words: thyroid gland • iodoproteins • endocytosis

Introduction

Thyroglobulin (Tg),[1] the precursor of the thyroid hormones triiodothyronine and thyroxine, derives from thyroid epithelial cells. Tg is mainly stored in thyroid follicle lumina, but is not restricted to the thyroid gland because it is also found in the circulation (1–3). Transepithelial vesicular transport (transcytosis) mediates passage of intact Tg from its storage compartment into the circulation (4–6). Clearance of Tg from the circulation occurs within the liver by endocytosis in Kupffer cells, i.e., macrophages (7). Internalization of Tg is accompanied by the proteolytic release of thyroid hormones from their precursor molecule (8). The biological significance of this extrathyroidal hormone release by macrophages might consist in paracrine interactions, e.g., with hepatocytes. Indeed, when hepatocytes and macrophages in coculture were incubated with Tg, the macrophages released thyroid hormones from their precursor molecule Tg, thereby stimulating the hepatocellular metabolism (7).

Because the level of Tg circulating in the blood is low (9–11), binding proteins for Tg must exist on macrophages to enable its specific recognition. However, so far no information exists on the nature of such Tg-binding proteins. Binding of Tg to the cell surface of thyroid epithelial cells is mediated by low-affinity receptors, which are saturated at high concentrations of Tg, i.e., 20 μM Tg (12). The putative receptor protein has a molecular mass of 46 kD, and exhibits a positive ligand cooperativity. Since Tg is known to carry mannose-6-phosphate moieties, it was assumed that the Tg-binding protein of thyrocytes might be identical to the cation-dependent mannose-6-phosphate receptor. However, further experiments showed that the 46-kD Tg-binding protein differed from the cation-dependent mannose-6-phosphate receptor (12). Another Tg-binding protein on thyroid epithelial cells is the so-called thyroid lectin (13), which is believed to mediate uptake of low-iodinated Tg molecules from the lumina of thyroid follicles (14). The thyroid lectin recognizes Tg molecules exposing *N*-acetylglucosamin in the terminal position of the *N*-linked glycans of Tg (13). It is believed to recycle low-iodinated Tg molecules via the Golgi apparatus to the apical plasma membrane, where Tg becomes available for iodination by the thyroid peroxidase and is released into the lumen of thyroid follicles (14).

Here we have analyzed the interaction of Tg with J774 cells with the aim to identify Tg-binding proteins on macrophages. By affinity chromatography, we have shown that Tg was recognized by two binding proteins on the cell surface of J774 macrophages. Unexpectedly, the Tg-binding proteins were identified as histone H1. We consider our findings physiologically relevant in that they explain uptake of circulating Tg by liver macrophages, which has been shown to result in the extra-

The current address of Wolfgang Summa is Data Trak Deutschland GmbH, Am Propsthof 80, D-53121 Bonn, Germany.

Address correspondence to Dr. Klaudia Brix, Institut für Zellbiologie, Universität Bonn, Ulrich-Haberland-Str. 61a, D-53121 Bonn, Germany. Phone: +49-228-735306; FAX: +49-228-735302; E-mail: brix@uni-bonn.de

Received for publication 27 August 1997 and accepted in revised form 1 May 1998.

J. Clin. Invest.
© The American Society for Clinical Investigation, Inc.
0021-9738/98/07/0283/11 $2.00
Volume 102, Number 2, July 1998, 283–293
http://www.jci.org

1. *Abbreviations used in this paper:* DTAF, 5-(4,6-dichlorotriazin-2-YL)-aminofluorescein hydrochloride; NHS, *N*-hydroxysuccinimide; PNGase F, peptide N-glycosidase F; RU, response units of the BIAcore™ 2000 system; SLE, systemic Lupus erythematosus; SML, sucrose monolaurate; Tg, thyroglobulin; TRITC, tetramethyl-rhodaminyl-isothiocyanate.

thyroidal release of thyroid hormones (8) and in the subsequent paracrine stimulation of the hepatocellular metabolism (7).

Methods

Cell culture

The murine macrophage-like cell line J774 A.1 (15) was obtained from American Type Culture Collection (Rockville, MD) and grown at 37°C and 5% CO_2 in DMEM (Bio-Whittaker, Serva, Heidelberg, Germany) supplemented with 10% heat-inactivated FCS, 100 IU/ml penicillin G, 0.1 mg/ml streptomycin, and 0.5 μg/ml amphothericin B.

Isolation and purification of Tg

Bovine thyroid glands were obtained from the local slaughterhouse, and were cut into small fragments. All of the following steps were performed at 4°C. For isolation of Tg, the tissue fragments were homogenized (Polytron™; Kinematica GmbH, Kriens, Switzerland) in PBS supplemented with protease inhibitors (1 mM *N*-α-p-tosyl-L-arginine methyl ester, 0.5 mM PMSF, 1 μg/ml antipain, 1 μg/ml pepstatin, 4 μg/ml aprotinin). After centrifugation (30 min at 22,000 *g*; Beckman Instruments, Inc., Fullerton, CA), the supernatant was subjected to fractionated ammonium sulfate precipitation (35% for 2 h and 45% overnight). The Tg fraction (45%) was dialyzed against 50 mM Tris-Cl, pH 7.4, and was further purified by anion-exchange chromatography using a MonoQ HR 5/5 column in a fast protein liquid chromatography device (Pharmacia LKB Biotechnology, Uppsala, Sweden). After elution with a linear NaCl gradient, the Tg fractions (0.4–0.8 M NaCl) were pooled and desalted (EconoPac™ 10DG; Bio-Rad Laboratories, Hercules, CA).

In vitro fluorochromation of Tg

Purified Tg (5–10 mg in 450 μl PBS) was incubated with 550 μl borate buffer (50 mM, pH 9.0) and 100 μl fluorochrome solution (5 mg of 5-[4,6-dichlorotriazin-2-YL]-aminofluorescein hydrochloride [DTAF] or of fluorescein isothiocyanate [FITC] per ml DMSO) for 4 h at room temperature, or overnight at 4°C. Free fluorochrome was removed by desalting (see above).

In vitro iodination of Tg

Iodination of 2 mg/ml Tg with [^{125}I]NaI was performed in PBS for 15 min at room temperature using iodobeads (Pierce, Oud-Beijerland, The Netherlands; 8, 16). Free [^{125}I]NaI was removed by desalting (see above), yielding specific radioactivities in the range of 150–400 cpm per ng protein. [^{125}I]Tg was used for quantitation of Tg-binding and Tg-internalization studies.

Production of polyclonal antibodies

Purified Tg was used to raise polyclonal antibodies (8) in rabbits according to standard protocols. Titers were 1:16 using 900 μg/ml Tg as an antigen in Ouchterlony analysis. Dilution (1:200) of the serum recognized 1 ng Tg in dot blots. The antibodies have been characterized previously (8).

Protein assay

Protein concentrations were determined according to Bradford (17). Lyophilized Tg or BSA were used as standards.

Fluorescence microscopy of Tg binding and internalization by J774 cells

Cells were grown on glass coverslides. For Tg binding, the macrophages were incubated for 30 min with DMEM supplemented with 200 nM Tg and fixed in methanol and acetone (each for 8 min, −20°C). After washing, cells were blocked with human IgG and ovalbumin before immunolabeling with rabbit anti-Tg and DTAF goat anti–rabbit Fab fragments of IgG (Dianova, Hamburg, Germany). For internalization of Tg, cells were incubated for 60 min with DMEM supplemented with 200 nM DTAF-Tg and fixed with 3% paraformaldehyde in PBS for 60 min. After washing and extraction with 0.5% Triton X-100 in PBS, the cortical F-actin system underneath the plasma membrane was labeled with 33 nM tetramethylrhodaminyl-isothiocyanate (TRITC)-coupled phalloidin.

Fluorescence microscopy of histone H1

For immunolabeling of histone H1 at the plasma membrane, J774 cells were fixed with 8% paraformaldehyde in 200 mM Hepes for 30 min, and were further treated for cryosectioning or immunolabeled without Triton X-100 treatment. After blocking (see above), cells or cryosections were immunolabeled with monoclonal anti-histone H1 antibodies (clone 5F3, see below; or clone AE-4; Leinco Technologies, Inc., Ballwin, MO; distributed by Biotrend, Köln, Germany) and FITC coupled to sheep anti-mouse F(ab′)$_2$-fragments (Sigma Chemical Co., St. Louis, MO).

Injection experiments and immunolabeling of liver cryosections

1 mg FITC-labeled bovine Tg dissolved in PBS was injected into mice via the vena cava inferior. After 12 min of incubation, mice were bled by opening the aorta descendens. Prewarmed PBS supplemented with heparin and 3% formaldehyde in 200 mM Hepes were perfused via the vena porta. The livers were dissected and postfixed with 8% formaldehyde in 200 mM Hepes, infiltrated with 2.3 M sucrose as a cryoprotectant, and frozen in liquid propane. As controls, livers from noninjected mice were prepared as described above. Sections were prepared with a cryotome (Reichert-Jung, Wien, Austria) at −50°C, and were mounted on microscope slides. Blocking was performed with human immunoglobulin G (Dianova, Hamburg, Germany) and ovalbumin. Cryosections were immunolabeled with anti-histone H1 monoclonal (clone AE-4; Leinco) and polyclonal (Fitzgerald Inds. Intl., Chelmsford, MA) antibodies and TRITC coupled to goat anti-mouse and donkey anti-sheep F(ab′)$_2$-fragments (Dianova).

Microscopy and documentation

Cells were mounted on microscope slides and viewed with a fluorescence microscope (Carl Zeiss, Inc., Oberkochen, Germany) equipped with filter sets suitable for double fluorescence. Cryosections or cells were also viewed with a confocal laser scanning microscope (TCS 4D; Leica, Bensheim, Germany) using an argon/krypton mixed-gas laser with excitation wavelengths of 488 and 568 nm. Scans at a resolution of 1024 × 1024 pixels and a pinhole setting of about 50 were taken in the line averaging mode. Micrographs were taken on Kodak TMax™ and EPY 64 T films™ (Eastman Kodak Co., Rochester, NY), or on Ilford Pan F films using a hardcopy device (Fokus Graphics, Oberau, Germany).

Affinity chromatographic analysis of Tg-binding proteins on J774 cells

All steps were performed at 4°C using a SMART™ system (Pharmacia Biotech, Inc., Uppsala, Sweden).

Coupling of Tg to N-hydroxysuccinimide (NHS)-activated superose. 100 pmol (66 μg) of purified Tg was coupled to *N*-hydroxysuccinimide–activated superose (PC 3.2/2; Pharmacia Biotech, Inc.) according to the standard protocol of the manufacturer. The same protocol was used to couple ethylamine to a control column. In brief, the superose matrices were activated with 6 vol of coupling buffer (0.1 M $NaHCO_3$, 0.5 mM NaCl, pH 8.3). Purified Tg (100 pmol) in coupling buffer was loaded onto the superose matrices and allowed to bind for 4 h. Nonbound ligands were removed by washing with 6 vol each of deactivating solution (1 M ethylamine, pH 8.0) and washing solution (0.1 M Na-acetate, 0.5 M NaCl, pH 5.0). After reequilibration in deactivating solution, the columns were incubated with ethylamine for 1 h and repeatedly washed with deactivating and washing solution to ensure complete blockage of free NHS groups. After washing with running buffer (50 mM Tris-Cl, 150 mM NaCl, 1 mM Na_2EDTA, 0.5% sucrose monolaurate, 0.03% NaN_3, pH 7.4), affinity matrices were stored at 4°C.

Cell surface biotinylation and preparation of cell lysates. After washing, 5 × 10^8 J774 cells were resuspended in 200 μg/ml biotinami-

docaproate *N*-hydroxysuccinimide ester (Sigma Chemical Co.) in PBS and incubated for 30 min on ice. Unbound biotin was removed by repeated washing in PBS containing 10 mM lysine. Cell surface biotinylated or nonbiotinylated cells were pelleted and lysed in 50 mM Tris-Cl (pH 7.4) supplemented with 0.5% sucrose monolaurate, 150 mM NaCl, 1 mM EDTA, and protease inhibitors (lysis buffer) for 1 h at 4°C with gentle agitation. The supernatant (10 min at 1,000 *g* and 1 h at 100,000 *g*; Beckman Instruments., Inc.) was analyzed by affinity chromatography.

Affinity chromatography on Tg-superose. Lysates from cell surface biotinylated or nonbiotinylated cells were loaded onto the Tg affinity column or onto the ethylamine control column at a flow rate of 100 μl/min. Unbound proteins were removed by washing with 10 vol of lysis buffer (see above). Bound proteins were eluted with lysis buffer containing 2 M NaCl, monitored at 254 and 280 nm, collected in fractions of 100 μl, and further analyzed by SDS-PAGE and blotting.

Affinity chromatography on heparin-sepharose. Lysates from cell surface–biotinylated cells were loaded onto HiTrap-heparin columns (Pharmacia Biotech, Inc.) and washed with 10 vol of lysis buffer followed by elution using a linear gradient of 0.15–2 M NaCl over 4 ml. Fractions of 100 μl were collected and further analyzed by SDS-PAGE and blotting.

Peptide N-glycosidase F (PNGase F) digestion. Eluates from the Tg affinity column were used either directly or after denaturation with SDS (0.5%, 5 min, 100°C), followed by the addition of 3% *N*-octylglucoside. Incubation with 40 μU PNGase F (Boehringer Mannheim GmbH, Mannheim, Germany) per μl of eluates was for 12 h at 37°C (pH 7.3) according to Tarentino et al. (18). Control incubations were performed identically but without adding PNGase F. Samples were then analyzed by SDS-PAGE and blotting.

SDS-PAGE and blotting

Samples were diluted in sample buffer (10 mM Tris/HCl [pH 7.6], 0.5% SDS, 25 mM DTT, 10% glycerol, 10 μg/ml bromophenolblue) and boiled for 3 min. Standard molecular mass markers for silver-stained gels were from Sigma Chemical Co. (Deisenhofen, Germany), and for Western blots rainbow marker kits (Amersham Buchler, Braunschweig, Germany) or biotinylated molecular mass markers (Sigma Chemical Co.) were used.

Samples were analyzed with a horizontal electrophoresis device (Pharmacia Biotech., Inc.) using gradient SDS-polyacrylamide gels (8–18%; 19). After electrophoresis, the gels were either fixed and silver-stained (20), or proteins were transferred to nitrocellulose (Schleicher & Schüll, Inc., Dassel, Germany) by Western blotting (21) using a semidry blotting chamber (Bio-Rad Laboratories). Unspecific binding sites were saturated in a solution containing 6% casein, 1% polyvinylpyrrolidon 40, and 10 mM EDTA in low-salt PBS (68 mM NaCl, 63 mM Na_2HPO_4, 12 mM NaH_2PO_4, pH 6.8). For detection of the biotin label, streptavidin coupled to HRP diluted in blocking solution was used. For immunological recognition of histone H1, monoclonal antibodies against histone H1 and secondary antibodies coupled to HRP (Dianova) were used. Monoclonal anti–histone H1 antibodies (clone AE-4) were from Fitzgerald Inds. Intl. (Chelmsford, MA). Monoclonal antibodies recognizing the highly conserved peptide sequence SGSFK at the COOH-terminal end of the globular core region of histone H1 (clone 5F3) were kindly provided by Drs. A. Steuernagel, B. Belgardt, and U. Grossbach (Göttingen, Germany). Streptavidin blots were developed in chloronaphthol as a substrate (21) or, as were immunoblots, by enhanced chemiluminescence. Documentation was on X-OMAT™ AR films (Eastman Kodak Co., Rochester, NY), which were further scanned using a transmitted light scanner (Hewlett-Packard, Palo Alto, CA) and documented on Ilford PanF films using a hardcopy device (see above).

Sequencing

Eluates from Tg affinity columns were separated on 8–18% SDS gels, and separated proteins were Coomassie-stained. Gel bands corresponding to the putative Tg binding proteins were dissected and cleaved in gel with Endoproteinase LysC (Boehringer Mannheim, Tutzing, Germany; 22). The generated peptides were eluted from the gel using extractions with 10% formic acid and with 100% acetonitrile. The eluates were combined, evaporated to dryness, redissolved in 3% formic acid, and subjected to reversed phase on a Superspher 60 RP Select B™ column (Merck, Darmstadt, Germany). Solvent A (0.1% trifluoroacetic acid in water) and solvent B (0.1% trifluoroacetic acid in acetonitrile) were used. A gradient was developed from 0–60% B in 60 min. Flow rate was 300 μl/min. The peptides were detected by UV absorption at 206 nm. Peptide-containing fractions were collected and subjected to NH_2-terminal amino acid sequence analysis using an ABI 492A amino acid sequencer (PE Applied Biosystems, Weiterstadt, Germany) according to the instructions of the manufacturer.

Extraction of histone H1 from J774 cells

For histone H1 extraction, the method of Johns (23) was used. Cells were washed and lysed before pelleting of the nuclei (10 min, 1,000 *g*). Thereafter, nuclei were subjected to 5% $HClO_4$ and extracted at 4°C for 30 min. Extracts were cleared by centrifugation (10 min, 14,000 *g*), and histone H1 was precipitated with 20% TCA for 2 h at 4°C. Precipitates were collected by centrifugation (20 min, 14,000 *g*), and were repeatedly washed with ice-cold acetone. Pellets were then air-dried in an evaporating chamber to remove acetone, and were stored at −20°C or boiled in sample buffer. The purity of such preparations was proven by SDS-PAGE and immunoblotting (not shown).

Interaction of Tg and histone H1 in vitro

The in vitro interaction between histone H1 extracted from J774 cells and Tg was analyzed by surface plasmon resonance using a BIAcore™ 2000 system (Biacore AB, Uppsala, Sweden). Tg was immobilized to CM5 sensor chips at a flow rate of 5 μl/min. Activation was for 12 min with a mixture (vol/vol) of 1-ethyl-3-(3-dimethylaminopropyl)carbodiimide and NHS. Coupling of 50 μg/ml Tg was for 12 s in 20 mM formic acid at pH 3.5 to a total of 550 response units (RU) followed by saturation with 1 M ethylamine for 12 min. After washing with HBS and a 2-min pulse of glycine at pH 3.0, the flow cell was equilibrated with HBS and PBS (pH 7.4). Analysis of the in vitro interaction of histone H1 with immobilized Tg was at a flow rate of 30 μl/min in PBS (pH 7.4). The Tg-loaded flow cell was equilibrated for 2 min before injection of histone H1 at various concentrations for 1 min. Dissociation phases of ~ 4 min were followed by regeneration with 10 mM HCl for 1 min and equilibration for 2.5 min. Recorded sensorgrams were evaluated with the BIA evaluation program (Biacore AB, version 3.0), and maximum RU during the association phases were plotted against the concentration of histone H1 using standard software (Microcal Origin 4.00; Microcal Software, Inc., Northampton, MA). The dissociation constants K_d were read out at half-maximum of binding as indicated in the plot.

Competition of plasma proteins with the in vitro interaction between histone H1 and Tg was analyzed by coinjection of 500 nM histone H1 and 5 nM to 500 μM of orosomucoid, fetuin, γ-globulins, transferrin, or heparin into the Tg-loaded flow cell. The running protocol, recording, and evaluation of sensorgrams was as described above. Binding of histone H1 alone was taken as 100%, and competition of plasma proteins coinjected with histone H1 was calculated as a percentage of histone H1 binding.

Quantitation of Tg binding and internalization

Binding of [^{125}I]Tg to J774 cells. Radioiodinated Tg was diluted with Tris buffer at pH 7.4 to give final concentrations ranging from 10 to 160 nM. Cells (2.5×10^7) were incubated in suspension for 60 min at 4°C with gentle agitation. Nonspecific binding was determined in the presence of 2 mg/ml nonradioactive Tg. Analysis was performed in duplicates. The cells were washed in PBS containing 1% BSA (five times, 100 *g* for 2 min). Final cell pellets were counted, and the amount of bound Tg was calculated and normalized using the DNA content as a measure of cell numbers.

Saturation and scatchard plot analysis. Measurements were analyzed according to Rosenthal (24), Bylund and Yamamura (25), and Marquardt (26) with standard computer software (Microcal Origin 2.94).

pH dependency of Tg binding. Cells were washed in incubation buffer (25 mM Tris, 25 mM bisTris) with pH values from 5.0 to 7.4, and were incubated for 60 min with 100 nM [^{125}I]Tg at 4°C. After repeated (six times) washing with incubation buffer supplemented with 1% BSA, the radioactivity of the pellets was counted. Bound Tg was calculated and normalized to DNA contents as described above.

Competition of Tg binding with heparin. Binding of 100 nM [^{125}I]Tg at 4°C was competed by adding 1 nM to 10 μM heparin (Braun Melsungen AG, Melsungen, Germany) to the incubation medium. Controls were incubated without heparin. Analysis was performed in triplicates. Washing and quantitation were as described above.

Internalization of [^{125}I]Tg by J774 cells. Cells were incubated with 100 nM [^{125} I]Tg in the presence of 50 nM to 2 μM nonradioactive Tg for 90 min at 37°C. Each incubation was performed in triplicates. Controls were performed without adding nonradioactive Tg. Washing and quantitation was as described above. To determine whether Tg-binding sites are internalized, cells were preincubated for 10 min with 100 nM nonradioactive Tg (pulse), and were further incubated for time intervals up to 240 min with incubation medium without Tg (chase) before incubation with 100 nM [^{125}I]Tg. In controls, preincubation with nonradioactive Tg was omitted. Washing and quantitation was as described above.

DNA content

Cell suspensions or the pellets from lysate clearing were used to determine the number of cells by measuring the DNA content (27).

Results

Isolation of Tg-binding proteins by affinity chromatography. J774 macrophages were incubated with Tg at various temperatures, fixed, and further processed for fluorescence microscopy. After incubation with Tg at 4°C and immunolabeling, a patched staining pattern was observed along the entire cell surface and at the filopodia of J774 macrophages (Fig. 1 *a*). Upon incubation of the macrophages with DTAF-labeled Tg for 60 min at 37°C, numerous fluorescent vesicles were detected (Fig. 1 *b*, *green*). The results indicated that Tg was bound to the plasma membrane of J774 macrophages at 4°C, and was internalized when incubations were done at 37°C. Because binding and endocytosis occurred at Tg concentrations as low as 30 nM, the presence of a Tg-binding protein at the cell surface of J774 macrophages was assumed.

To test this hypothesis by affinity chromatography, Tg was immobilized on a superose column, and ethylamine–superose matrices were used as controls. Lysates of J774 cells were passed over the columns, and elution with high salt revealed several proteins that bound to the Tg affinity column (Fig. 2, lane *3*). As compared with the protein pattern of cell lysates (Fig. 2, lane *1*), two proteins with an apparent molecular mass of ~ 33 kD were highly enriched in the eluates of the Tg affinity column (lane *3*). These proteins were not eluted from control columns (Fig. 2, lane *2*), indicating their avidity to Tg. The electrophoretic mobility of the two protein bands enriched in the eluates from Tg affinity columns was the same in SDS gels run under reducing or nonreducing conditions (not shown), indicating that they were not linked by disulfide bonds.

To investigate whether these two proteins were localized at the plasma membrane, J774 macrophages were cell surface–biotinylated at 4°C before cell lysis and analysis by affinity chromatography. Biotinylation was omitted in control experiments. The eluates from the Tg affinity column were separated on SDS-gels, and were silver-stained or transferred to nitrocellulose (Fig. 3). When the blots were probed with peroxidase-labeled streptavidin, two Tg-binding proteins were identified as plasma membrane constituents (Fig. 3, lane *4*). They had the same electrophoretic mobility as the two proteins enriched in the nonbiotinylated control eluates from the affinity column (Fig. 3, compare lane *2* with lane *1*). Digestion of the eluates from the Tg affinity column with PNGase F did not increase

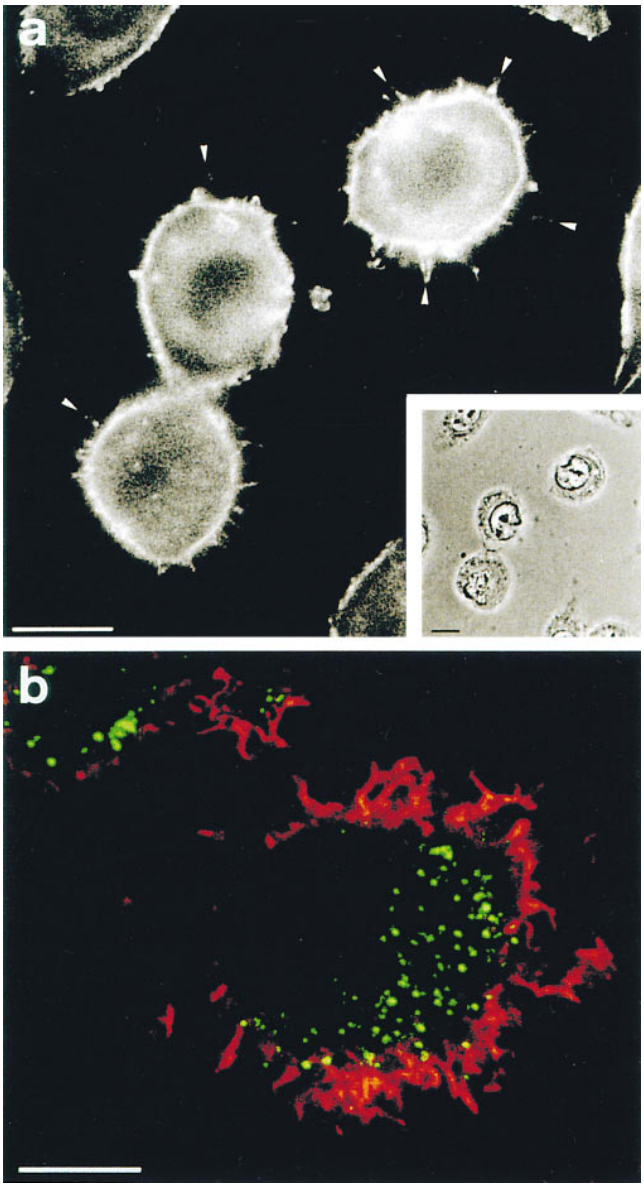

Figure 1. Binding and endocytosis of Tg by J774 macrophages. (*a*) Conventional immunofluorescence and corresponding phase contrast (*inset*) micrographs demonstrating Tg binding to J774 macrophages. Cells were incubated with Tg at 4°C, and were immunolabeled with antibodies against Tg. Binding of Tg to J774 cells occurred along the entire cell surface and at filopodia (*arrowheads*). (*b*) Confocal fluorescence micrograph of J774 macrophages after internalization of DTAF-Tg at 37°C (*green*) and phalloidin-labeling of the cortical F-actin system (*red*). DTAF-Tg was internalized and accumulated within lysosomes of J774 cells. *Bars*, 10 μm.

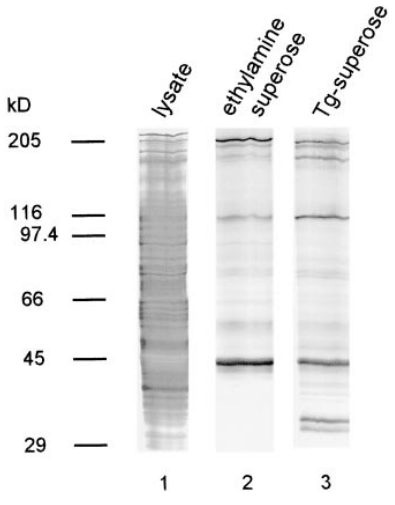

Figure 2. Identification of Tg binding proteins by affinity chromotography. SDS-PAGE and subsequent silver staining of cell lysates (lane *1*) and eluates from a Tg superose affinity column (lane *3*), or an ethylamine control column (lane *2*). Several proteins were eluted from Tg affinity columns with two of them being highly enriched (lane *3*) when compared with eluates from the control column (lane *2*). The two proteins from J774 cells with a high avidity for Tg (lane *3*) had apparent molecular masses of ~ 33 kD.

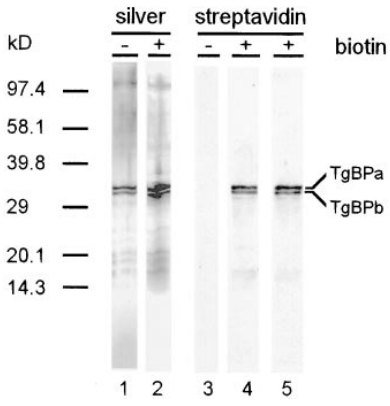

Figure 3. Cell surface biotinylation of Tg-binding proteins. Proteins at the plasma membrane of J774 cells were biotinylated at 4°C (lanes *2*, *4*, and *5*) before analysis of the cell lysates by affinity chromatography on Tg superose. Biotinylation was omitted in control experiments (lanes *1* and *3*). SDS-PAGE and silver staining of eluates from Tg-superose columns revealed Tg binding proteins with similar electrophoretic mobility before (lane *1*) and after cell surface biotinylation (lane *2*). Western blotting and streptavidin detection of the biotin label demonstrated the presence of Tg-binding proteins at the cell surface of the macrophages (lane *4*). Digestion of the eluates from the Tg affinity column with PNGase F (lane *5*) suggested that the two Tg-binding proteins (TgBPa and TgBPb) were not *N*-glycosylated.

their electrophoretic mobility (Fig. 3, lane *5*), suggesting that the two Tg-binding proteins were not *N*-glycosylated. In addition, blots from eluates of the Tg-affinity column were probed with a glycoprotein detection kit, demonstrating that the Tg-binding proteins were not glycosylated (not shown).

The results demonstrated that two proteins present at the plasma membrane of J774 cells bound to immobilized Tg, and thus were likely candidates for Tg-binding proteins (TgBPa and TgBPb as indicated in Fig. 3).

Identification of TgBPs as histone H1. Eluates of the Tg affinity column were concentrated by ultrafiltration, separated on SDS gels, and blotted onto PVDF membranes to identify the TgBPs. Edman degradation of the two protein bands representing TgBP a or b did not result in any signal, indicating that the NH_2 termini of both proteins were blocked. Therefore, TgBP a and b were dissected from Coomassie-stained SDS gels and digested with endoproteinase Lys-C. Resulting peptides were eluted with TFA and separated by reversed-phase chromatography. Edman degradation of two peptides derived from TgBPa resulted in identification of the sequences ASGPPVSELITK and ALAAAGYDVE. Both sequences were identical to regions within the highly conserved globular domains of mouse histones H1.1 and H1.5, rat histone H1.2, or human histones H1C and H1D (Fig. 4).

Histone H1 has a molecular mass of 22 kD, which clearly contrasted with the apparent molecular mass of ~ 33 kD for TgBP a and b. Because of its positively charged amino acids, histone H1 has a slower electrophoretic mobility on SDS gels than expected, resulting in bands slightly above the 30-kD molecular mass marker (28). Hence, from the sequencing experiments we concluded that TgBPa is identical to histone H1.

Two monoclonal antibodies against histone H1, i.e., clones 5F3 and AE-4, were used for immunolabeling experiments. The monoclonal antibody AE-4 stained nuclei in cryosections from J774 cells (Fig. 5, *a* and *a′*) as was expected, because histone H1 is a nuclear antigen. In addition, a weak immunoreaction of AE-4 with the cell surface was also observed (Fig. 5 *a′*, *arrowheads*). To verify the labeling of histone H1 at the cell surface, cells were fixed and immunolabeled without further Triton X-100 treatment. The monoclonal antibody AE-4 recognized patches on the cell surface (Fig. 5, *b* and *b′*), suggesting the presence of cell surface–associated histone H1 in nonpermabilized cells. Similar results were obtained when the monoclonal antibody 5F3 recognizing a highly conserved peptide sequence within the globular domain of most H1 histones was used for immunolabeling nonpermeabilized J774 cells (not shown). Furthermore, histone H1 was heavily labeled with the antibody AE-4 in condensed, and therefore most probably apoptotic, cells (Fig. 5, asterisks in *c*, *c′* and *c′′*) and at the cell surface of their direct neighbors (Fig. 5, *arrowhead* in *c′′*). This

TgBPa		ASGPPVSELITK ALAAAGYDVE
H1.1 (mouse)	28-AGVRRK	ASGPPVSELITKAVAASKERSGVSLAALKKALAAAGYDVEKNNSRIKL-81
H1.5 (mouse)	29-AAGKRK	ASGPPVSELITKAVAASKERSGVSLAALKKALAAAGYDVEKNNSRIKL-82
H1.2 (rat)	28-GGAKRK	ASGPPVSELITKAVAASKERSGVSLAALKKALAAAGYDVEKNNSRIKL-81
H1B (human)	28-GAAKRK	ASGPPVSELITKAVAASKERSGVSLAALKKALAAAGYDVEKNNSRIKL-81
H1C (human)	28-AGARRK	ASGPPVSELITKAVAASKERSGVSLAALKKALAAAGYDVEKNNSRIKL-81
H1D (human)	27-GGTPRK	ASGPPVSELITKAVAASKERSGVSLAALKKALAAAGYDVEKNNSRIKL-80

Figure 4. Identification of TgBPa as histone H1 by peptide sequencing. Sequencing experiments revealed the identity of two peptides derived from TgBPa (*first line*) with sequences within the highly conserved region of histone H1 from mouse, rat, or human origins. Sequences are given in the one-letter code for amino acids. Underlining indicates the position of the highly conserved globular domain of histone H1.

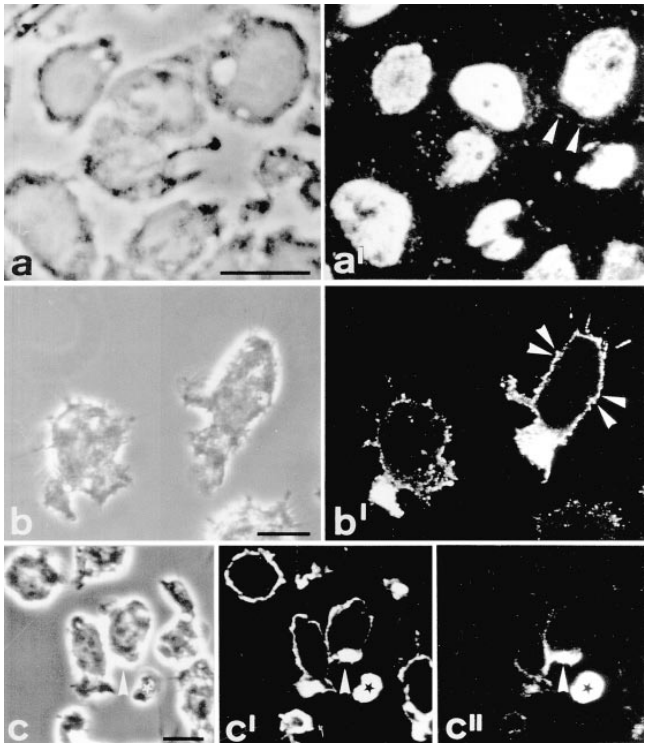

Figure 5. Immunocytochemical detection of histone H1 at the cell surface. Confocal fluorescence (*a′*, *b′*, *c′*, and *c′′*) and corresponding phase contrast micrographs (*a*, *b*, and *c*) of paraformaldehyde-fixed J774 cells. Cryosections (*a* and *a′*) or nonpermeabilized cells (*b* to *c′′*) were stained with the monoclonal anti-histone H1 antibody AE-4 (*a′*, *b′*, and *c′′*) or polyclonal antibodies against J774 plasma membrane proteins (*c′*) and DTAF-labeled secondary antibodies. Histone H1 was detected within the nuclei of J774 cells (*a′*), as was expected. In addition, cell surface–associated histone H1 was weakly stained in cryosections (*arrowheads* in *a′*). The cell surfaces (*arrowheads* in *b′* and *c′′*) and condensed cells (*asterisks* in *c* to *c′′*) were strongly stained with anti-histone H1 antibodies when fixed cells were immunolabeled without further permeabilization. Histone H1 was associated with the cell surface of J774 macrophages in a patched pattern (*b′*). *Bars*, 10 μm.

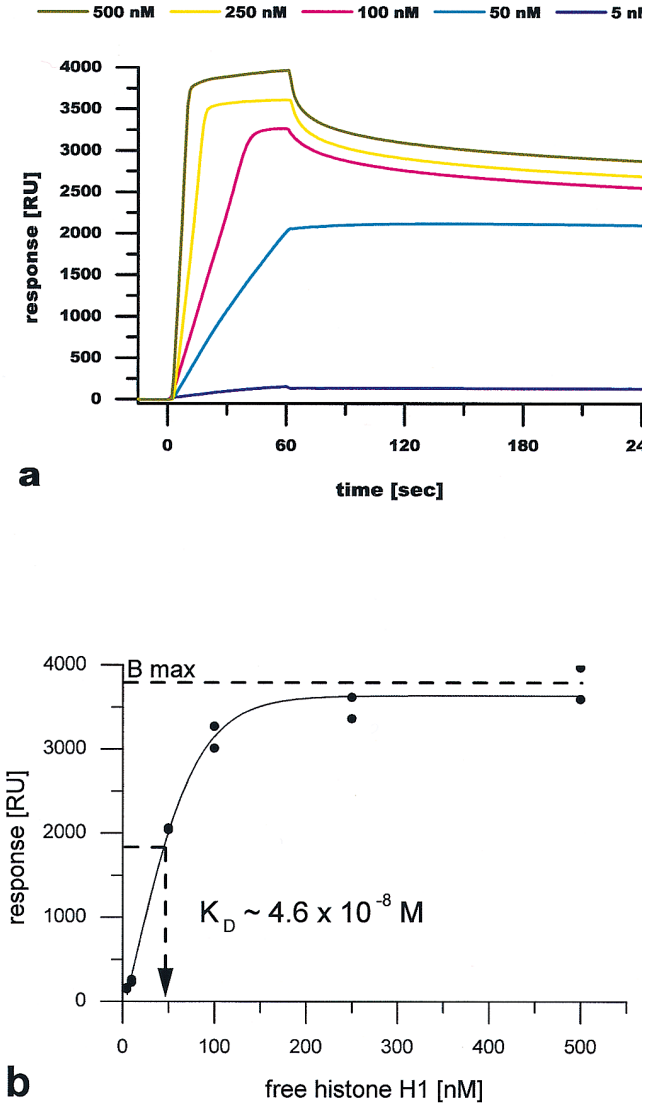

Figure 6. Surface plasmon resonance analysis of the in vitro interaction of histone H1 and Tg. Binding of histone H1 extracted from nuclei to immobilized Tg was investigated by surface plasmon resonance. Sensorgrams of single experiments are given as overlays (*a*) and were used to determine the maximum of histone H1 binding in response units (RU) during the association phases (0–60 s). Plots of RU against the concentration of free histone H1 (*b*) showed that binding of histone H1 to Tg is saturable with a dissociation constant of $\sim 4.6 \times 10^{-8}$ M.

result suggested that dead cells released histone H1, which in a secondary event associated with the cell surface of neighboring cells. The staining of patches of cell surface–associated histone H1 (Fig. 5 *b′*) was similar to the staining pattern observed after incubation of the cells with Tg (cf. Fig. 1 *a*), indicating that the binding of Tg and histone H1 at the plasma membrane of J774 cells was similar. The results suggested that histone H1 at the cell surface of J774 macrophages served as a binding protein for Tg.

In vitro interaction of histone H1 with Tg. Since histone H1 at the cell surface of J774 macrophages was assumed as a binding protein for Tg, the interaction of both proteins was analyzed in vitro by means of surface plasmon resonance. Rapid association and dissociation was observed when histone H1 extracted from J774 cells interacted with immobilized Tg (Fig. 6 *a*). When the maximum responses during the association phases were plotted against the concentration of free histone H1, a saturation kinetic was detected (Fig. 6 *b*). The results indicated that histone H1 and Tg interacted in vitro with a dissociation constant in the nanomolar range, i.e., 4.6×10^{-8} M.

Solutions containing saturating amounts of histone H1, i.e., 500 nM, supplemented with increasing amounts of fetuin, γ-globulins, heparin, orosomucoid, or transferrin as competitors for histone H1 were analyzed by surface plasmon resonance to determine the specificity of histone H1 binding to immobilized Tg. Molar ratios of 0.01–1,000 between competing proteins and histone H1 were analyzed. When transferrin or orosomucoid were used as competitors, no inhibition of histone H1 binding to immobilized Tg was observed (Fig. 7, *squares*). Fetuin or γ-globulins competed with histone H1 binding to Tg, however, inhibition did not exceed 65% (not

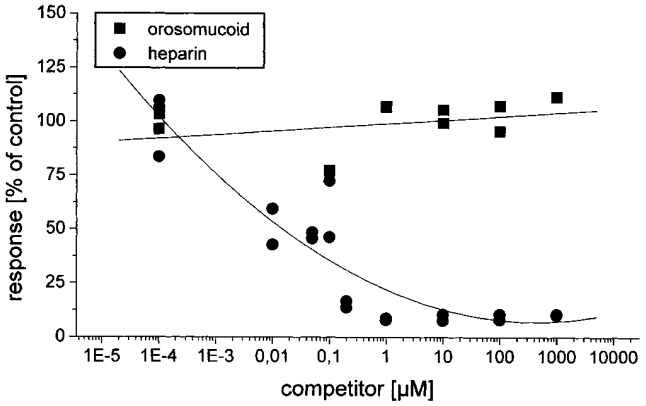

Figure 7. Competition of the in vitro interaction of histone H1 and Tg by heparin. Competition of orosomucoid or heparin with the in vitro interaction of histone H1 and Tg was investigated by surface plasmon resonance. Competition was analyzed by adding increasing amounts of orosomucoid (*squares*) or heparin (*circles*) to solutions containing 500 nM histone H1, and binding is given as the percentage of the control, i.e., binding of histone H1 alone. Using orosomucoid as a competitor revealed no inhibition (*squares*), whereas increasing amounts of heparin progressively competed for the binding of histone H1 to immobilized Tg (*circles*).

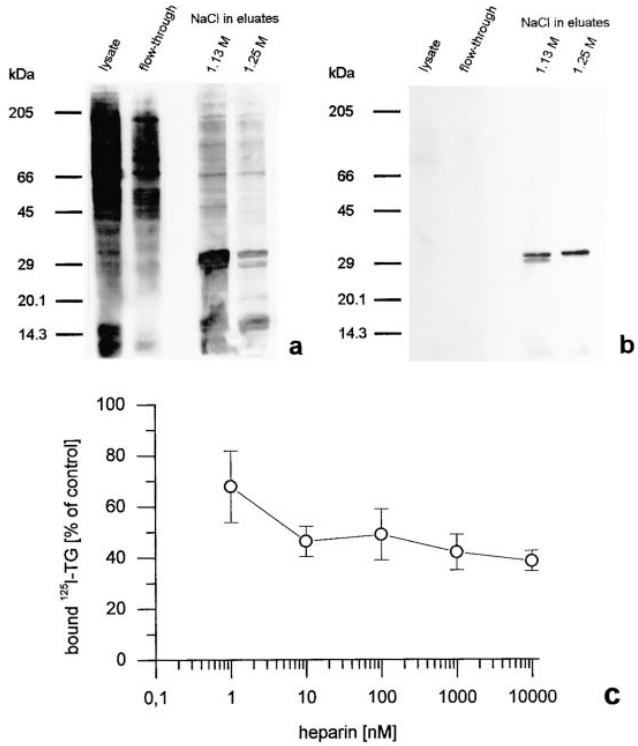

Figure 8. Inhibition of Tg binding by heparin. (*a* and *b*) SDS-PAGE and streptavidin detection of cell surface–biotinylated proteins (*a*) or immunodetection of histone H1 (*b*) in eluates from heparin affinity columns. Streptavidin detection revealed the binding of a doublet at ~ 33 kD to heparin columns that was eluted with 1.13 M NaCl (*a*, 1.13 M). This doublet was recognized as histone H1 by specific antibodies probed to Western blots of eluates from the heparin affinity column (*b*), indicating that cell surface–associated histone H1 bound to heparin. (*c*) Cells were incubated with radioiodinated Tg at 4°C in the presence of increasing amounts of heparin, resulting in inhibition of Tg binding. The results indicated that heparin serves as an inhibitor of Tg binding to J774 cells by interfering with the interaction between Tg and the Tg binding protein histone H1.

shown). In contrast, when heparin was used as a competitor for histone H1 binding to immobilized Tg, increasing amounts of inhibition were observed with a maximum of ~ 90% inhibition at molar ratios of 1–1,000 between heparin and histone H1 (Fig. 7, *circles*). The results demonstrated that the in vitro binding of histone H1 to immobilized Tg was specific. In addition, heparin was shown to compete efficiently with the in vitro interaction of histone H1 and Tg.

Heparin is an effective inhibitor of Tg binding to the surface of J774 macrophages. Because it is known that heparin interacts with histone H1, and because it competed with the in vitro interaction of histone H1 and Tg (see above), we assumed heparin to be an effective inhibitor of Tg endocytosis by J774 macrophages. To verify the interaction of heparin with histone H1 at the cell surface of macrophages, lysates of cell surface–biotinylated J774 cells were passed over heparin columns. The eluted fractions were transferred to nitrocellulose, and blots were probed with HRP-streptavidin to visualize cell surface proteins that bound to heparin (Fig. 8 *a*). Two biotinylated protein bands with an apparent molecular mass of ~ 33 kD were eluted from the heparin column with 1.13–1.25 M NaCl (Fig. 8 *a*). These two proteins were identified as histone H1 by immunoblotting (Fig. 8 *b*), indicating that cell surface–associated histone H1 from J774 macrophages interacts in vitro with heparin. To test whether heparin influences the interaction of Tg with histone H1 in vivo, J774 cells were incubated with radioiodinated Tg at 4°C, and with increasing amounts of heparin in the incubation media. Cell-bound radioactivity was reduced to 50% of control values (100%) by adding 10 nM heparin to the incubation media (Fig. 8 *c*). The molar ratio of heparin and Tg needed to achieve 50% inhibiton of Tg binding was 1:10. When increasing the ratio of heparin to Tg, inhibition slightly increased, however, it did not exceed 60% inhibition of Tg binding to J774 cells (Fig. 8 *c*). The results indicated that heparin serves as an inhibitor of Tg binding to J774 cells by interfering with the interaction between Tg and the TgBP histone H1.

Characterization of Tg binding to J774 cells. To characterize Tg binding, J774 cells were incubated with radioiodinated Tg with or without 3 µM nonradioactive Tg at 4°C. In the absence of nonradioactive Tg, the amount of cell-bound [^{125}I]Tg increased with increasing amounts of free Tg exhibiting a saturation kinetic (Fig. 9 *a*, *open circles*, *broken line*). In the presence of nonradioactive Tg , the cell-bound radioactivity was lower, and increased in a linear manner (Fig. 9 *a*, *triangles*, *unbroken line*). The specific binding of [^{125}I]Tg to the surface of J774 cells was calculated (Fig. 9 *b*) by subtracting nonspecific binding (Fig. 9 *a*, *triangles*) from total binding (Fig. 9 *a*, *open circles*). Saturation of specific Tg binding to J774 cells was reached at values of ~ 100 nM Tg (Fig. 9 *b*). Rosenthal–Scatchard plot analysis revealed a dissociation constant of ~ 5×10^{-8} M with 5,700 functional binding sites per cell (Fig. 9 *c*). The results indicated the existence of a limited amount of Tg-binding sites present on the surface of J774 cells.

Internalization of radioiodinated Tg at 37°C was inhibited by adding increasing amounts of unlabeled Tg to the incuba-

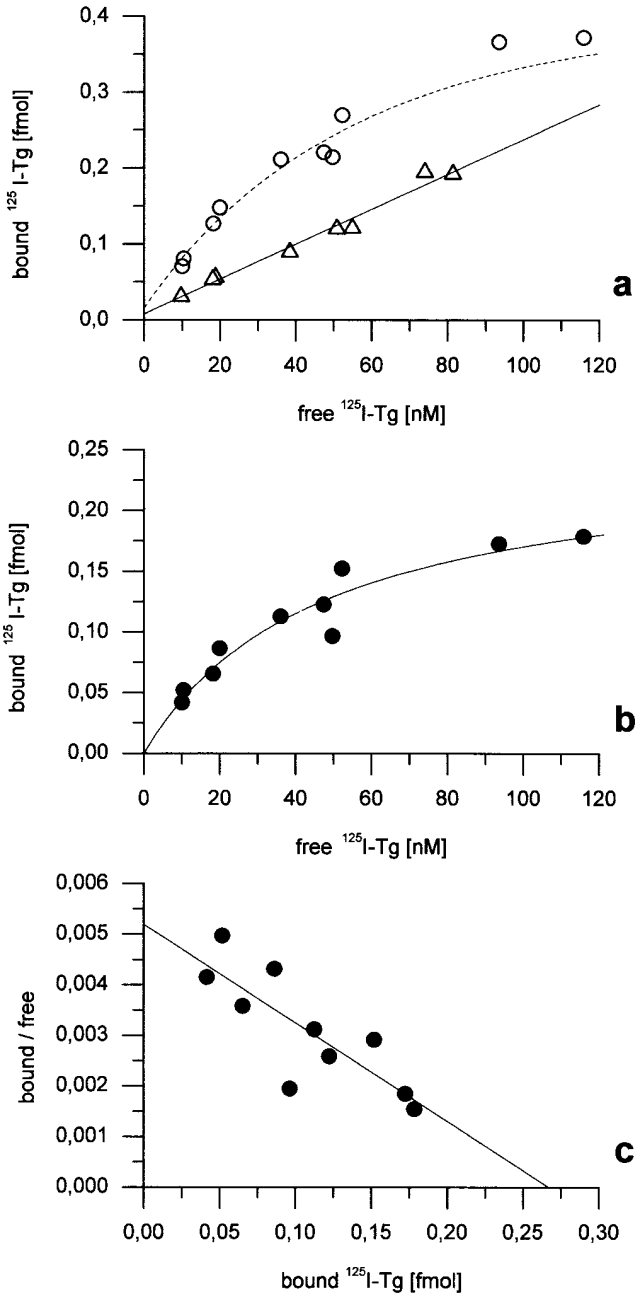

Figure 9. Saturation of Tg binding. J774 cells were incubated with increasing amounts of radioiodinated Tg at 4°C (*a*) in the presence (*triangles*) or absence (*circles*) of 2 mg/ml nonradioiodinated Tg. Nonspecific binding (*a*, *triangles*) was subtracted from total binding (*a*, *circles*) to give specific binding of Tg to J774 cells (*b*, *filled circles*). The amount of bound Tg increased with increasing amounts of free Tg, and was saturable at ~ 100 nM Tg (*b*). Rosenthal-Scatchard plot analysis demonstrated a dissociation constant of $\sim 5 \times 10^{-8}$ M (*c*) with 5,700 functional binding sites per cell.

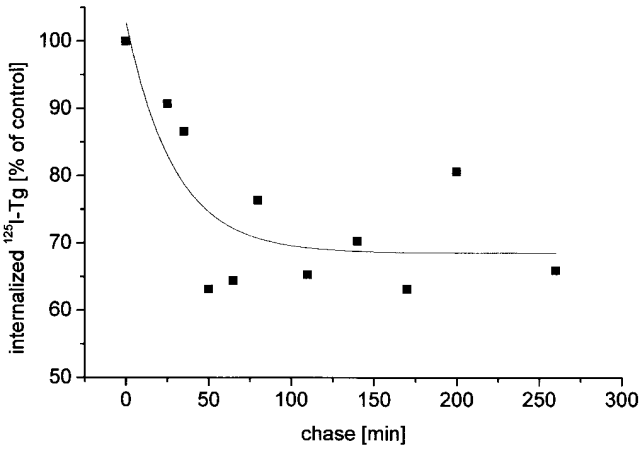

Figure 10. Rapid internalization of Tg binding sites. J774 cells were incubated with nonradioactive Tg for 10 min (pulse) and chased in Tg-free media for the indicated time intervals (chase). To determine the ability of cells to bind Tg, macrophages were then incubated with radioiodinated Tg for 10 min. Preincubation of J774 cells with Tg resulted in the disappearance of Tg binding sites because the amounts of internalized radioiodinated Tg decreased with prolonged chase times. Maximum inhibition of [^{125}I]Tg internalization was observed after 50 min of chase. The results indicated that Tg binding sites were internalized by J774 cells during the 10-min pulse, and were not recycled within 260 min of chase.

tion media (not shown). Similarly, preincubation of J774 cells with Tg in pulse-chase experiments diminished the amount of internalized Tg by ~ 40% after 50 min of chase (Fig. 10). Up to 260 min of chase, the amount of internalized Tg increased again; however, it did not reach control values (Fig. 10). The results indicated that binding sites for Tg were rapidly removed from the cell surface during internalization of Tg. Binding sites for Tg were not recycled within 4 h.

These findings implied that binding of Tg to histone H1 is stable at acidic pH, i.e., after internalization within early endocytic compartments. To test this prediction, J774 cells were incubated with radioiodinated Tg at various pH values in the incubation media. Tg binding to the surface of J774 cells was stable at pH values ranging from 6.5 to 7.5, and was even stronger at pH values below 6.5 (not shown). Similarly, binding of histone H1 to Tg affinity columns was stable at acidic pH values (not shown). Since the isoelectric points of Tg and histone H1 are 4.5 and 8.4, respectively, it can be assumed that both proteins were oppositely charged within physiological pH ranges. Thus, the results suggested that the binding of Tg as a ligand for H1 is brought about by ionic interactions.

Colocalization of internalized Tg with histone H1 in mouse liver macrophages. The findings on J774 cells suggested that histone H1 at the cell surface of macrophages mediated internalization of Tg, and therefore should be present in Tg-containing endocytic compartments of macrophages. To test this prediction in vivo, FITC-labeled Tg was injected into mice, and cryosections of livers from noninjected or injected animals were immunolabeled with anti-histone H1 antibodies.

Immunolabeling of cryosections from livers of noninjected animals with anti-histone H1 antibodies visualized nuclear histone H1 in all liver cells and vesicular histone H1 mainly in macrophages (Fig. 11 *b*, *red*). In addition, a weak immunoreactivity was observed at the cell surface of liver macrophages (Fig. 11 *b*, *red*, *arrowhead*).

The injected FITC-Tg accumulated within vesicles of macrophages, indicating that Kupffer cells of the liver mediated endocytosis of circulating Tg (Fig. 11 *d*, *green*). For identification of Tg-internalizing cells as liver macrophages, see Brix et al., 1997 (7). Immunolabeling with anti-histone H1 antibod-

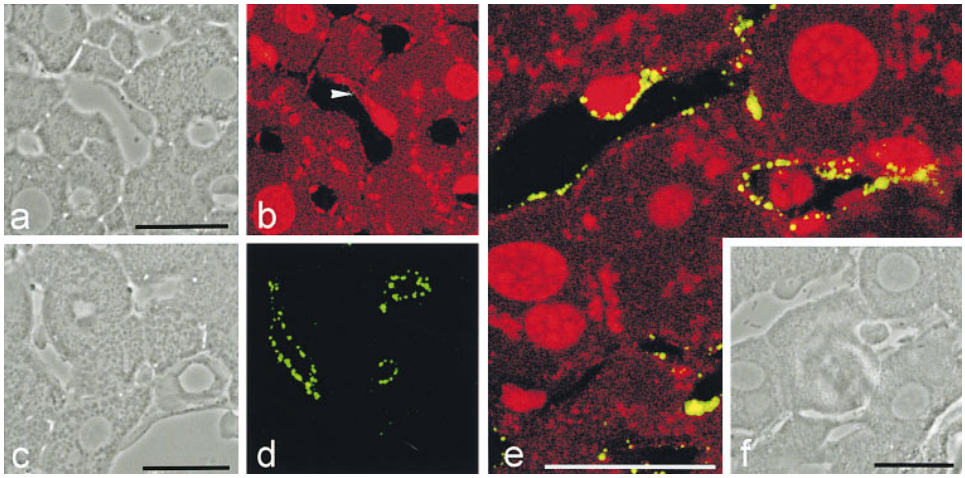

Figure 11. Immunocytochemical detection of histone H1 within endocytic compartments of liver macrophages. Confocal fluorescence (*b*, *d*, and *e*) and corresponding phase contrast micrographs (*a*, *c*, and *f*) of cryosections through mouse livers. The micrographs in *a* and *b* are from tissue of noninjected mice, and the micrographs in *c–f* are from tissue fixed 12 min after injection of FITC-labeled Tg. Fluorescent Tg was internalized by Kupffer cells, i.e., macrophages of the liver (*d* and *e*, *green*). Cryosections were immunolabeled with monoclonal and polyclonal anti-histone H1 antibodies and TRITC-labeled secondary antibodies (*b* and *e*, *red*). In controls, anti-histone H1 antibodies were omitted (*d*), demonstrating the specificity of the antibodies against histone H1 by the absence of any red signal. Nuclear histone H1 and histone H1 within endocytic vesicles of liver macrophages were recognized by anti-histone H1 antibodies (*red* in *b* and *e*). In addition, a weak immunoreactivity of anti-histone H1 antibodies with the cell surface of liver macrophages of noninjected animals was observed (*arrowhead* in *b*). Note the colocalization of histone H1 (*red*) and FITC-Tg (*green*) within endocytic compartments of liver macrophages (yellow signals as a result of overlapping red and green signals in *e*), suggesting histone H1–mediated internalization of Tg by liver macrophages in vivo. *Bars*, 25 μm.

ies revealed staining of vesicular histone H1 colocalizing with FITC-Tg–containing vesicles (Fig. 11 *e*, *yellow* as a result of overlapping red histone H1 signals and green FITC-Tg signals), and that of nuclear histone H1 (Fig. 11 *e*, *red*). Controls performed by omitting primary anti-histone H1 antibodies were negative (Fig. 11 *d*, green signals are derived from FITC-Tg), demonstrating the specificity of anti-histone H1 antibodies.

These results suggested that histone H1 is not restricted to nuclear compartments of liver cells, rather, that histone H1 is also found colocalized with the internalized FITC-Tg within endocytic vesicles of liver macrophages, supporting the notion that histone H1 indeed mediated internalization of Tg by macrophages in vivo.

Discussion

Histone H1 serves as a Tg-binding protein on the cell surface of macrophages. The aim of this study was to identify binding sites for Tg at the cell surface of macrophages. Binding of Tg to J774 macrophages was saturable with a dissociation constant of receptor ligand complexes of ~ 50 nM. Tg binding on J774 cells resulted in rapid uptake of Tg by endocytosis. Recycling of the Tg-binding protein was not observed. Affinity chromatography on immobilized Tg and subsequent sequencing of the binding partners for Tg as well as immunolabeling experiments identified histone H1 as the Tg-binding protein on the cell surface of J774 macrophages. Furthermore, colocalization of Tg and histone H1 within endocytic compartments of liver macrophages suggested that histone H1 also mediated internalization of Tg by liver macrophages in vivo. Surface plasmon resonance analysis of the in vitro interaction between Tg and histone H1 revealed a dissociation constant of 46 nM, similar to the dissociation constant for Tg binding on cell surfaces. Since Tg (p.I. 4.5) and histone H1 (p.I. 8.4) are oppositely charged at physiological pH, Tg binding to histone H1 at the cell surface of J774 macrophages is most probably brought about by ionic interactions. The interaction of histone H1 with the plasma membrane of J774 cells is as of yet unclear.

Identification of histone H1 as a Tg-binding protein on the cell surface of macrophages was unexpected because histones are considered to be restricted to nuclear locations. Within the nuclei, histone H1 is located in the interior of the 30-nm chromatin fibers (29). Whereas the core histones H2A, H2B, H3, and H4 form the nucleosomes, histone H1 shows a more peripheral localization, and together with histone H5 is often referred to as the linker histone (30, 31). The nuclear function of histone H1 comprises not only structural features, but also implies a specific function for histone H1 in regulating gene expression (32–35). Histone H1 shows an enormous microheterogeneity of subtypes (33, 36–42) and different degrees of posttranslational modifications (43) such as phosphorylation, resulting in a multiple banding pattern on SDS gels (34, 43). The sequencing data of the Tg-binding protein on J774 cells do not allow us to predict precisely the subtype of histone H1. The sequences of the upper band of the Tg-binding protein (TgBPa)–derived peptides were, however, identical in the overlapping region with the histone variants H1.1 and H1.5. Immunologically, nuclear and cell surface–bound histone H1 in J774 cells were indistinguishable. The source of histone H1 that reaches the plasma membrane of J774 cells is still unknown (see below).

Cell surface localization of histones. A common theme of eukaryotic cells is the targeting of a given protein to a specific compartment within the cell. However, evidence is accumulating that some proteins have multicompartmentalized isoforms (44, 45). One prominent example is Mac-2, a nuclear transcription factor of colon epithelial and HeLa cells, which has another function: Mac-2 is a well-characterized cell surface receptor of leukocytes (45–47). Similarly, nuclear transcription factors with homeodomains become secreted before being taken up by neighboring cells where they affect gene transcription in a paracrine fashion (48).

Besides these examples, it became obvious in the past that the core histones H2A, H2B, H3, and H4 are frequently detected at the cell surface of leukocytes or endothelial cells (49–59). The question on how histones reach the plasma membrane and how they are anchored at the cell surface remains a matter of debate. Several authors have forwarded the idea that the histones derived from dead cells during cell culture, which were then bound to receptors at the cell surface or complexed to one another (53, 56, 57, 59, 60). As yet, histone H1 was not described at the cell surface of leukocytes. However, the heparin-binding proteins HSBP1A and HSBP1B at the plasma membrane of human lung carcinoma cells were similar to histones H2A and H2B, and most importantly, a doublet with a molecular mass of 32 kD, i.e., the heparin-binding proteins HSBP2A and HSBP2B (55), show similarities to histone H1. Here we have described the binding of Tg to histone H1 at the cell surface of mouse macrophages and the interaction of heparin with histone H1. In addition, heparin proved to be a potent inhibitor of Tg binding to J774 cells, thus supporting the view that it is indeed histone H1 that is the binding protein for Tg at the cell surface.

Biological implications of histones on the cell surface. The proposed functions of histones and other nuclear material at the plasma membrane of leukocytes reaches from a protective role against perforin-mediated cell lysis (56) to a function in the removal of nuclear material from the extracellular spaces at sites of inflammation or cell death (57). Obviously, nucleosomes or DNA and other nuclear material bind to various proteins on the cell surface of leukocytes (61–66), i.e., receptors with apparent molecular masses of 30 kD (61, 65). Disorders in the removal of nuclear material from extracellular spaces might lead to induction of autoimmune diseases such as systemic Lupus erythematosus (SLE), where autoantibodies against nuclear material are frequently found (57, 67). Such disorders in the removal of nuclear material might arise because of the dysfunctioning or absence of the respective DNA receptors on leukocytes (57, 65, 68). Antibodies against histones might cause this dysfunctioning of the DNA receptors (68), indicating the importance of histones for binding nuclear material to leukocytes. Besides a further and direct role of histones in the induction of inflammation and tissue damage in Lupus nephritis (69), involvement of MHC class II presentation of peptides derived from histones was shown to induce Lupus in mice (67, 70), suggesting internalization and proteolytic processing of histones in antigen-presenting leukocytes. Autoantibodies against histones in autoimmune diseases such as SLE or axonal neuropathy comprise not only antibodies against the core histones (71), but also those against the linker histone H1 (72, 73).

In addition to its function as a Tg-binding protein, histone H1 might also function in endocytosis, since binding sites were rapidly removed from the cell surface of J774 macrophages, and because histone H1 was detected immunologically within Tg-containing endocytic compartments of mouse liver macrophages. Thus, internalization of the receptor ligand complexes might result in their proteolytic breakdown within endocytic compartments of the macrophages. As a result, presentation of histone H1 and Tg breakdown products at the plasma membrane of macrophages is conceivable. Proteolytic cleavage of Tg by J774 cells results in rapid liberation of thyroid hormones from the prohormone Tg (8). In this respect, a case report may be of specific interest, because not only anti-Tg autoantibodies, but also anti-T3 autoantibodies were observed in a patient suffering from SLE (74).

In conclusion, histone H1 on the cell surface of macrophages serves as a binding protein for Tg internalization. This process provides an explanation for the extrathyroidal release of thyroid hormones by macrophages (8), and the subsequent initiation of paracrine interactions between macrophages and hepatocytes (7).

Acknowledgments

The authors are grateful to Dr. U. Grossbach (Göttingen, Germany) and Dr. W. Neumüller for critical reading of the manuscript. Special thanks to Drs. U. Grossbach, A. Steuernagel, B. Belgardt, and J.R. Wisniewski (Göttingen, Germany) for providing the monoclonal antibody 5F3, and to Dr. K.E. Howell (Denver, CO) for providing the antiserum against J774 proteins. We wish to thank Dr. B. Haase (Biacore AB, Freiburg, Germany) for his advice during analysis of the in vitro interaction of histone H1 and Tg by surface plasmon resonance.

K. Brix was a recipient of a Lise-Meitner grant from the Ministerium für Wissenschaft und Forschung des Landes Nordrhein-Westfalen, IB3-6037. The work was supported by Deutsche Forschungsgemeinschaft, SFB 284, and by Fonds der Chemischen Industrie.

References

1. Hjort, T. 1961. Determination of serum-thyroglobulin by a haemagglutination-inhibition test. *Lancet.* 1:1262–1264.

2. Roitt, I.M., and G. Torrigiani. 1967. Identification and estimation of undegraded thyroglobulin in human serum. *Endocrinology*. 81:421–429.

3. Van Herle, A.J., and D.G. Brown. 1990. Thyroglobulin in benign and malignant thyroid disease. *In* Thyroid Disease: Endocrinology, Surgery, Nuclear Medicine, and Radiotherapy. S.A. Falk, editor. Raven Press, Ltd., New York. 473–484.

4. Herzog, V. 1983. Transcytosis of thyroid follicle cells. *J. Cell Biol.* 97: 607–617.

5. Herzog, V. 1984. Pathways of endocytosis in thyroid follicle cells. *Int. Rev. Cytol.* 91:107–139.

6. Romagnoli, P., and V. Herzog. 1991. Transcytosis in thyroid follicle cells: regulation and implications for thyroglobulin transport. *Exp. Cell Res.* 194:202–209.

7. Brix, K., R. Wirtz, and V. Herzog. 1997. Paracrine interaction between hepatocytes and macrophages after extrathyroidal proteolysis of thyroglobulin. *Hepatology*. 26:1232–1240.

8. Brix, K., and V. Herzog. 1994. Extrathyroidal release of thyroid hormones from thyroglobulin by J774 mouse macrophages. *J. Clin. Invest.* 93:1388–1396.

9. Uller, R.P., A.J. Van Herle, and I.J. Chopra. 1973. Comparison of alterations in circulating thyroglobulin, triiodothyronine and thyroxine in response to exogenous (bovine) and endogenous (human) thyrotropin. *J. Clin. Endocrinol. Metab.* 37:741–745.

10. Van Herle, A.J., H. Klandorf, and R.P. Uller. 1975. A radioimmunoassay for serum rat thyroglobulin. Physiologic and pharmacological studies. *J. Clin. Invest.* 56:1073–1081.

11. De Baets, M.H., A.M. Janssens, C.G. Romball, and W.O. Weigle. 1983. A radioimmunoassay for murine thyroglobulin in serum: age-related increase of serum thyroglobulin levels in AKR/J mice. *Endocrinology.* 112:1788–1795.

12. Lemansky, P., and V. Herzog. 1992. Endocytosis of thyroglobulin is not mediated by mannose-6-phosphate receptors in thyrocytes. Evidence for low-affinity-binding sites operating in the uptake of thyroglobulin. *Eur. J. Biochem.* 209:111–119.

13. Thibault, V., O. Blanck, J. Courageot, C. Pachetti, C. Perrin, A. de-Mascarel, and R. Miquelis. 1993. The *N*-acetylglucosamine-specific receptor of the thyroid: purification, further characterization, and expression patterns on normal and pathological glands. *Endocrinology*. 132:468–476.

14. Miquelis, R., J. Courageot, A. Jacq, O. Blanck, C. Perrin, and P. Bastiani. 1993. Intracellular routing of GLcNAc-bearing molecules in thyrocytes: selective recycling through the Golgi apparatus. *J. Cell Biol.* 123:1695–1706.

15. Ralph, P., J. Prichard, and M. Cohn. 1975. Reticulum cell sarcoma: an effector cell in antibody-dependent cell-mediated immunity. *J. Immunol.* 114: 898–905.

16. Markwell, M.A.K. 1982. A new solid-state reagent to iodinate proteins. I. Conditions for the efficient labeling of antiserum. *Anal. Biochem.* 125:427–432.

17. Bradford, M.M. 1976. A rapid and sensitive method for the quantitation of microgram quantities of protein using the principle of protein-dye binding. *Anal. Biochem.* 72:248–254.

18. Tarentino, A.L., C.M. Gomez, and T.H. Plummer, Jr. 1985. Deglycosylation of asparagine-linked glycans by peptide:*N*-glycosidase F. *Biochem. J.* 24: 4665–4671.

19. Laemmli, U.K. 1970. Cleavage of structural proteins during the assembly of the head of bacteriophage T4. *Nature*. 227:680–685.

20. Heukeshoven, J., and R. Dernick. 1988. Improved silver staining procedure for fast staining in PhastSystem development unit. I. Staining of sodium dodecyl sulfate gels. *Electrophoresis*. 9:28–32.

21. Towbin, H., T. Staehelin, and J. Gordon. 1979. Electrophoretic transfer of proteins from polyacrylamide gels to nitrocellulose sheets: procedure and some applications. *Proc. Natl. Acad. Sci. USA*. 76:4350–4354.

22. Eckerskorn, C., and F. Lottspeich. 1989. Internal amino acid sequence analysis of proteins separated by gel electrophoresis after tryptic digestion in polyacrylamide matrix. *Chromatographia*. 28:92–94.

23. Johns, E.W. 1977. The isolation and purification of histones. *Methods Cell Biol.* 16:183–203.

24. Rosenthal, H.E. 1967. A graphic method for the determination and presentation of binding parameters in a complex system. *Anal. Biochem*. 20:525–532.

25. Bylund, D.B., and H.I. Yamamura. 1990. Methods for receptor binding. *In* Methods in Neurotransmitter Analysis. H.I. Yamamura, editor. Raven Press, Ltd., New York. 1–35.

26. Marquart, D.W. 1963. An algorithm for least squares estimation of nonlinear parameters. *J. Soc. Indust. Appl. Math*. 11:431–441.

27. Burton, K. 1956. A study of the conditions and mechanism of the diphenylamine reaction for the colorimetric estimation of desoxyribonucleic acid. *Biochem. J.* 62:315–323.

28. Grunwald, D., J.J. Lawrence, and S. Khochbin. 1995. Accumulation of histone $H1^0$ during early *Xenopus laevis* development. *Exp. Cell Res.* 218:586–595.

29. Graziano, V., S.E. Gerchman, D.K. Schneider, and V. Ramakrishnan. 1994. Histone H1 is located in the interior of the chromatin 30-nm filament. *Nature*. 368:351–354.

30. Pruss, D., J.J. Hayes, and A.P. Wolffe. 1995. Nucleosomal anatomy—where are the histones? *Bioessays*. 17:161–170.

31. Burley, S.K., X. Xie, K.L. Clark, and F. Shu. 1997. Histone-like transcription factors in eukaryotes. *Curr. Opin. Struct. Biol.* 7:94–102.

32. Wolffe, A.P. 1994. Transcription: in tune with the histones. *Cell*. 77:13–16.

33. Grossbach, U. 1995. Selective distribution of histone H1 variants and high mobility group proteins in chromosomes. *Sem. Cell Biol.* 6:237–246.

34. Dimitrov, S., and A.P. Wolffe. 1996. Remodeling somatic nuclei in *Xenopus laevis* egg extracts: molecular mechanisms for the selective release of histones H1 and $H1^0$ from chromatin and the acquisition of transcriptional competence. *EMBO* (*Eur. Mol. Biol. Organ.*) *J.* 15:5897–5906.

35. Shen, X., and M.A. Gorovsky. 1996. Linker histone H1 regulates specific gene expression but not global transcription in vivo. *Cell.* 86:475–483.

36. Wells, D., and C. McBride. 1989. A comprehensive compilation and alignment of histones and histone genes. *Nucl. Acids Res*. 17(Suppl.):311–346.

37. Schulze, E., S. Nagel, K. Gavenis, and U. Grossbach. 1994. Structurally divergent histone H1 variants in chromosomes containing highly condensed interphase chromatin. *J. Cell Biol.* 127:1789–1798.

38. Berger, R.G., R. Hoffmann, M. Zeppezauer, W. Agner-Redeker, L. Maljers, A. Ingendoh, and F. Hillenkamp. 1995. Separation and characterisation of bovine histone H1 subtypes by combined ion-exchange and reversed-phase chromatography and mass spectrometry. *J. Chromatogr*. 711:159–165.

39. Cole, R.D. 1987. Microheterogeneity in H1 histones and its consequences. *Int. J. Pept. Protein Res.* 30:433–449.

40. Khochbin, S., and A.P. Wolffe. 1994. Developmentally regulated expression of linker-histone variants in vertebrates. *Eur. J. Biochem.* 225:501–510.

41. Schulze, E., L. Trieschmann, B. Schulze, E.R. Schmidt, S. Pitzel, K. Zechel, and U. Grossbach. 1993. Structural and functional differences between histone H1 sequence variants with differential intranuclear distribution. *Proc. Natl. Acad. Sci. USA*. 90:2481–2485.

42. Wisniewski, J.R., and U. Grossbach. 1996. Structural and functional properties of linker histones and high mobility group proteins in polytene chromosomes. *Int. J. Dev. Biol.* 40:177–187.

43. Wu, R.S., H.T. Panusz, C.L. Hatch, and W.M. Bonner. 1986. Histones and their modifications. *CRC Crit. Rev. Biochem*. 20:201–263.

44. Danpure, C.J. 1995. How can the products of a single gene be localized to more than one intracellular compartment? *Trends Cell Biol.* 5:230–238.

45. Smalheiser, N.R. 1996. Proteins in unexpected locations. *Mol. Biol. Cell.* 7:1003–1014.

46. Lotz, M.M., C.W. Andrews, Jr., C.A. Korzelius, E.C. Lee, G.D. Steele, Jr., A. Clarke, and A.M. Mercurio. 1993. Decreased expression of Mac-2 (carbohydrate binding protein 35) and loss of its nuclear localization are associated with the neoplastic progression of colon carcinoma. *Proc. Natl. Acad. Sci. USA*. 90:3466–3470.

47. Dagher, S.F., J.L. Wang, and R.J. Patterson. 1995. Identification of galectin-3 as a factor in pre-mRNA splicing. *Proc. Natl. Acad. Sci. USA*. 92:1213–1217.

48. Prochiantz, A., and L. Theodore. 1995. Nuclear/growth factors. *Bioessays*. 17:39–44.

49. Rekvig, O.P., and K. Hannestad. 1977. Certain polyclonal antinuclear antibodies cross-react with the surface membrane of human lymphocytes and granulocytes. *Scand. J. Immunol*. 6:1041–1054.

50. Rekvig, O.P., and K. Hannestad. 1980. Human autoantibodies that react with both cell nuclei and plasma membranes display specificity for the octamer of histones H2A, H2B, H3, and H4 in high salt. *J. Exp. Med.* 152:1720–1733.

51. Rekvig, O.P., and K. Hannestad. 1981. Lupus erythematosus (LE) factors recognize both nucleosomes and viable human leucocytes. *Scand. J. Immunol.* 13:597–604.

52. Horneland, M., O.P. Rekvig, L. Jorgensen, and K. Hannestad. 1983. Cultured human endothelial cells display an antigen that is recognized by certain human anti-chromatin autoantibodies. *Clin. Exp. Immunol.* 54:373–377.

53. Holers, V.M., and B.L. Kotzin. 1985. Human peripheral blood monocytes display surface antigens recognized by monoclonal antinuclear antibodies. *J. Clin. Invest.* 76:991–998.

54. Rekvig, O.P., S. Muller, J.P. Briand, B. Skogen, and M.H. Van Regenmortel. 1987. Human antinuclear autoantibodies crossreacting with the plasma membrane and the *N*-terminal region of histone H2B. *Immunol. Invest*. 16: 535–547.

55. Bilozur, M.E., and C. Biswas. 1990. Identification and characterization of heparan sulfate-binding proteins from human lung carcinoma cells. *J. Biol. Chem.* 265:19697–19703.

56. Ojcius, D.M., S. Muller, C.S. Hasselkus Light, J.D. Young, and S. Jiang. 1991. Plasma membrane-associated proteins with the ability to partially inhibit perforin-mediated lysis. *Immunol. Lett.* 28:101–108.

57. Emlen, W., V.M. Holers, W.P. Arend, and B. Kotzin. 1992. Regulation of nuclear antigen expression on the cell surface of human monocytes. *J. Immunol.* 148:3042–3048.

58. Mecheri, S., G. Dannecker, D. Dennig, P. Poncet, and M.K. Hoffmann. 1993. Anti-histone autoantibodies react specifically with the B cell surface. *Mol. Immunol.* 30:549–557.

59. Watson, K., R.J. Edwards, D.C. Parmelee, S. Shaunak, N.J. Gooderham, and D.S. Davies. 1994. Histones located on the plasma membrane of T-cells. *Biochem. Soc. Trans*. 22:199S.

60. Rekvig, O.P. 1989. Intrinsic cell membrane antigens recognized by anti-chromatin autoantibodies. The membrane antigens do not derive from the nucleus. *Scand. J. Immunol.* 29:7–13.

61. Bennett, R.M., G.T. Gabor, and M.M. Merritt. 1985. DNA binding to human leukocytes. Evidence for a receptor-mediated association, internalization, and degradation of DNA. *J. Clin. Invest.* 76:2182–2190.

62. Jacob, L., M.A. Lety, R.C. Monteiro, F. Jacob, J.F. Bach, and D. Louvard. 1987. Altered cell-surface protein(s), crossreactive with DNA, on spleen cells of autoimmune lupic mice. *Proc. Natl. Acad. Sci. USA*. 84:1361–1363.

63. Loke, S.L., C.A. Stein, X.H. Zhang, K. Mori, M. Nakanishi, C. Subasinghe, J.S. Cohen, and L.M. Neckers. 1989. Characterization of oligonucleotide transport into living cells. *Proc. Natl. Acad. Sci. USA*. 86:3474–3478.

64. Bennett, R.M., K.A. Cornell, M.J. Merritt, A.C. Bakke, P.H. Hsu, and S.H. Hefeneider. 1991. Autoimmunity to a 28–30 kD cell membrane DNA binding protein: occurrence in selected sera from patients with SLE and mixed connective tissue disease (MCTD). *Clin. Exp. Immunol.* 86:374–379.

65. Bennett, R.M., J.S. Peller, and M.M. Merritt. 1986. Defective DNA-receptor function in systemic lupus erythematosus and related diseases: evidence for an autoantibody influencing cell physiology. *Lancet*. 1:186–188.

66. Emlen, W., A. Rifai, D. Magilavy, and M. Mannik. 1988. Hepatic binding of DNA is mediated by a receptor on nonparenchymal cells. *Am. J. Pathol.* 133:54–60.

67. Kotzin, B.L. 1996. Systemic Lupus erythematosus. *Cell*. 85:303–306.

68. Bennett, R.M., B.L. Kotzin, and M.J. Merritt. 1987. DNA receptor dysfunction in systemic lupus erythematosus and kindred disorders. Induction by anti-DNA antibodies, antihistone antibodies, and antireceptor antibodies. *J. Exp. Med*. 166:850–863.

69. Schmiedeke, T.M., F.W. Stockl, R. Weber, Y. Sugisaki, S.R. Batsford, and A. Vogt. 1989. Histones have high affinity for the glomerular basement membrane. Relevance for immune complex formation in lupus nephritis. *J. Exp. Med.* 169:1879–1894.

70. Mohan, C., S. Adams, V. Stanik, and S.K. Datta. 1993. Nucleosome: a major immunogen for pathogenic autoantibody-inducing T cells of lupus. *J. Exp. Med.* 177:1367–1381.

71. Kotzin, B.L., J.A. Lafferty, J.P. Portanova, R.L. Rubin, and E.M. Tan. 1984. Monoclonal anti-histone autoantibodies derived from murine models of lupus. *J. Immunol.* 133:2554–2559.

72. Ravirajan, C.T., S. Muller, D.R. Katz, and D.A. Isenberg. 1995. Effect of histone and histone-RNA complexes on the disease process of murine systemic lupus erythematosus. *Autoimmunity*. 21:117–122.

73. Brindel, I., J.L. Preud'homme, J.J. Diaz, C. Giraud, J.M. Vallat, and M.O. Jauberteau. 1995. A human monoclonal IgM lambda specific for an epitope shared by the 200 kDa neurofilament protein, histones and ribosomal proteins. *J. Autoimmun*. 8:915–929.

74. Sakata, S., T. Komaki, S. Nakamura, S. Suzuki, K. Torigai, M. Kojima, and K. Miura. 1987. A case of systemic Lupus Erythematosus (SLE) and Sjögren's syndrome associated with anti-T3 autoantibodies. *Endocrinol. Jpn*. 34:497–503.